The reflectivity and photoconductivity spectra of $Cd_{1-x}Fe_xTe$ in the 1.0–30.0 eV energy range

D Dębowska†, M Zimnal-Starnawska†, A Rodzik†, A Kisiel†, M Piacentini‡, N Zema§ and W Giriat¶

† Institute of Physics, Jagellonian University, Reymonta 4, 30059 Cracow, Poland
‡ Dipartimento di Energetica, Università degli Studi di Roma, via A Scarpa 14, 00161 Roma, Italy
§ Istituto di Struttura della Materia del CNR, via E Fermi 38, 00044 Frascati, Italy
¶ Instituto Venezolano de Investigationes Cientificas, Centro de Fisica, Apartado 1827, Caracas 1010A, Venezuela

Abstract. The reflectivity and photoconductivity spectra for mixed crystals $Cd_{1-x}Fe_xTe$ ($0.00 \leqslant x \leqslant 0.05$) have been investigated. The reflectivity measurements have been carried out in a wide energy range—1.0–30.0 eV at 300 and 77 K. The photoconductivity spectra have been taken in the 1.0–3.0 eV range at 300 K. The analysis of the energy positions of maxima in reflectivity and photoconductivity spectra as a function of the Fe concentration allowed us to confirm the existence of the deep donor-like state predicted by the band-structure model of these compounds. Using the photoconductivity data, the value of 0.08 eV above the top of the valence band for the energy position of this deep donor-like state was found. The influence of $Fe^{2+}(3d^6)$ states on the changes in the energy positions of the reflectivity maxima E_0, E_1, $E_1 + \Delta_1$, E_2, E_1', $E_1' + \Delta$, c, d, e, f, h and i has been analysed and the results obtained are consistent with the models existing in the literature.

1. Introduction

The mixed crystals $Cd_{1-x}Fe_xTe$ belong to the group of materials known as 'diluted magnetic semiconductors' (DMSs). Because of their important semiconducting and magnetic properties [1], DMSs have recently been the subject of extensive studies. These ternary systems contain magnetic atoms that randomly replace some of cations in the II–VI semiconductor lattice. While the intrinsic properties of Mn-based DMSs are now reasonably well understood, the situation is quite different in the case of Fe-based DMSs. The predominant part of the physical properties of the DMS, in our case CdTe with Fe, depends on the location of the $Fe^{2+}(3d^6)$ states relative to the top of the valence band (VB) or to the bottom of the conduction band (CB). In general, the $Fe^{2+}(3d^6)$ level is much higher in the band structure of the host crystal than the $Mn^{2+}(3d^5)$ level that is well below the top of the VB [2]. The first studies of the optical absorption of $Cd_{1-x}Fe_xTe$ were carried out by Joshi and Mogollón [3]. They found that with increasing Fe content the absorption edge shifts to lower energies and also that a rich structure around the absorption edge can be seen. This structure was interpreted by them as transitions between the states of the Fe^{2+} ion (d → d transitions), in a similar way to the Mn-based II–VI compounds.

At the conference in West Berlin in 1985 Kisiel *et al* [4] presented the first reflectivity results obtained for $Cd_{1-x}Fe_xTe$ samples in the 0.5–6.0 eV energy range. They observed a non-linear dependence of the energy positions of the maxima on Fe concentration. Sarem *et*

al [5–7] presented some optical data for the DMSs (CdTe, CdSe and HgSe) with Fe taken in the 1–12 eV energy range. They observed changes in the shapes of the measured reflectivity spectra, caused by the influence of the Fe content. The experimental results were compared with the calculated band structure of the host crystals [8, 9]. Their results have contributed to the models [10–12] of the electronic structure of these compounds.

The photoemission studies carried out by Taniguchi *et al* [10] for $Cd_{1-x}Mn_xTe$ supplied arguments for creating a band-structure model for these crystals. Taking this into consideration and using the fundamental reflectivity measurements for $Cd_{1-x}Fe_xSe$, Kisiel *et al* [11] presented a one-electron schematic diagram of the splitting and hybridization of $Fe^{2+}(3d^6)$ states in $Cd_{1-x}Fe_xSe$. According to this model the Fe^{2+} ($3d^6$) level splits into spin-up ($d^5\uparrow$) and spin-down ($d^1\downarrow$) states by the exchange interaction. Each of these states is further split by the crystal field (of symmetry T_d in the zincblende structure) into a doublet e and a triplet t_2. In the lattice with T_d symmetry the occupied t_2 states hybridize with p-like anion states, giving the main contribution near the top of the VB. The e states remain localized. According to Mycielski *et al* [13], the ($d^1\downarrow$), acting as a deep donor, should appear as a state close to the top of the VB. Soon after, Taniguchi *et al* [12] suggested a slightly different model for $Cd_{1-x}Fe_xSe$, assigning the structure present in their photoemission spectra at 0.5 eV below the top of the VB, to the e spin-down ($d^1\downarrow$) state. Very recently Sarem *et al* [5, 7], on the basis of existing models and their optical-reflectivity studies for $Cd_{1-x}Fe_xTe$, introduced a model of p–d hybridization for the $A_{1-x}^{II}Fe_xB^{VI}$ wide-gap zincblende DMS. They located the e spin-down ($d^1\downarrow$) state above the top of the VB in agreement with the model for $Cd_{1-x}Fe_xSe$ [11]. This state, acting as a deep donor in $Cd_{1-x}Fe_xTe$, has been located in the forbidden energy gap at ~ 0.15 eV above the top of the VB [6]. Lischka *et al* [14], on the basis of their photo-EPR results for CdTe with very small substitutional Fe concentration, obtained a level identified as a deep donor. The ionization energy of this state, corresponding to the Fe^{2+} (d^6) $\rightarrow$ Fe^{3+} (d^5) + CB electron transition, has been determined to be 1.45 eV [15], i.e. about 0.1 eV above the VB maximum (VBM). Also the photoconductivity measurements for CdTe doped with Fe (Fe concentration $\sim 3 \times 10^{18}$ cm^{-3}) performed by Szadkowski [16] confirm the existence of an $Fe^{2+/3+}$ donor state lying about $0.13 - 0.15$ eV above the VBM and the value of the ionization energy as 1.455 eV.

In this paper we present the reflectivity measurements and the photoconductivity studies performed for the $Cd_{1-x}Fe_xTe$ ternary systems for $0.001 \leqslant x \leqslant 0.05$ Fe content. The dependence of the maximum energy position E_0 on Fe concentration, resulting from both methods, allows us to confirm and extend the model of the electronic structure for these materials. The influence of $Fe^{2+}(3d^6)$ states and their s–p–d hybridization with the bands of the host crystal makes it possible to explain the behaviour of the changes in the shape and the energy positions of the other maxima in reflectivity spectra.

2. Experiment

The ternary system $Cd_{1-x}Fe_xTe$ crystallizes in the zincblende structure for $x \leqslant 0.06$ [2] with the Fe^{2+} ions replacing Cd^{2+} at random lattice sites. The incompatibility of the NiAs structure, in which FeTe crystallizes, with the zincblende structure of CdTe imposes an upper limit for x.

The monocrystalline samples of $Cd_{1-x}Fe_xTe$ used in our studies were prepared by the modified Bridgman method using individual elements as starting materials. The samples were cleaved and their surfaces were cleaned with methyl alcohol just before the experiment.

In figure 1 the calibration curve presenting the linear dependence of the lattice constant, determined at room temperature from x-ray diffraction using the Debye–Scherrer method, as a function of the concentration x of Fe, checked by microprobe (precision better than 0.001), is shown. Taking into account the results for the measured lattice constant and the presented calibration curve the Fe content for the samples studied is as follows: $x = 0.0, 0.001, 0.01, 0.03$, and 0.05. The linear dependence mentioned above is different from those indicated in [6]. Such discrepances might be attributed to different resolutions of the experimental techniques used.

The reflectivity measurements for the $Cd_{1-x}Fe_xTe$ crystals were carried out in the 1–30 eV energy range while the photoconductivity spectra were taken only in the infrared and visible regions. The measurement procedures and experimental apparatus for the reflectivity experiment in the energy range 1–6 eV are described elsewhere [17]. The measurements were taken using conventional light sources with a resolution better than 0.01 eV. The reflectivity measurements were performed at 300 K (RT) and 77 K (LNT). The photoconductivity was measured at RT only, using the same set-up modified according to the suggestion given in [17], with the modulated beam light (modulation frequency equal to 12 Hz) in the constant collecting electric field. The ohmic electrical contacts for the photoconductivity measurements were achieved by evaporated gold. The crystals showed a good photoresponse and their resistance was of the order of 10^5–10^6 Ω. The reflectivity measurements above 5 eV were carried out at RT with the use of synchrotron radiation available at the vacuum ultraviolet beam line at the PULS facility in Frascati [18]. The average resolution of the set-up was 1–2 Å over the entire energy range.

3. Results and discussion

The reflectivity spectra of $Cd_{1-x}Fe_xTe$ in the energy range between 1 and 30 eV are presented in figure 2. The shapes of the spectra were affected by the sample quality and the surface preparation. Variations as large as ± 0.01 eV of the energies of the reflectivity structures have been noticed while studying different samples. In order to clarify the details of the reflectivity structure and to make the analysis more convenient the results are divided into three energy ranges: 1–6 eV, 6–11 eV, and 11–30 eV.

3.1. The 1–6 eV energy range

A selected group of the reflectivity spectra of $Cd_{1-x}Fe_xTe$ at RT and LNT are shown in figure 3(a) and (b), respectively. The main maxima for pure CdTe denoted in Cardona's notation as E_0, E_1, $E_1 + \Delta_1$, and E_2, are marked by arrows. With increasing Fe concentration, there are some changes in the shapes and energy positions of the maxima and also in their relative intensities. For the Fe concentration used in our investigation the blurring of the reflectivity structure, which occurs for CdTe with Mn [19–22], is not observed and all the peaks are well pronounced. In figure 4(a) and (b) the dependences of the reflectivity maxima energy positions on the Fe content are presented at RT and LNT, respectively. Figure 5(a) shows the photoconductivity curves for mixed $Cd_{1-x}Fe_xTe$ and pure CdTe, for comparison. The first maximum E_p observed in the photoconductivity, and the E_0 feature in the reflectivity spectrum of pure CdTe, are associated with the lowest interband transition between the top of the VB (Γ_8) and the bottom of the CB (Γ_6) at the Γ point in the Brillouin zone. For $Cd_{1-x}Fe_xTe$ the energy positions of E_p and E_0 are not the same because of the different initial state; E_0 is still the transition from the top of the VB to the bottom of the CB while E_p becomes the transition from the highest occupied
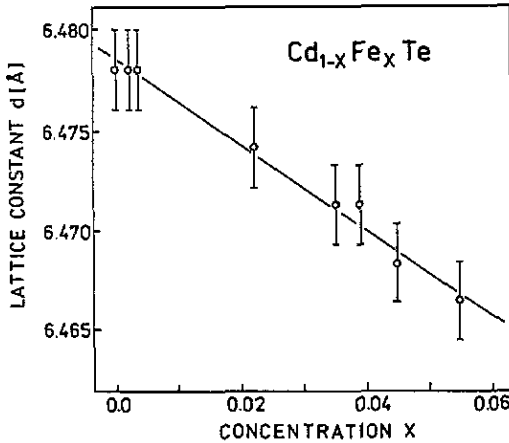
Figure 1. The dependence of the lattice constant on the Fe concentration for mixed crystals $Cd_{1-x}Fe_xTe$.

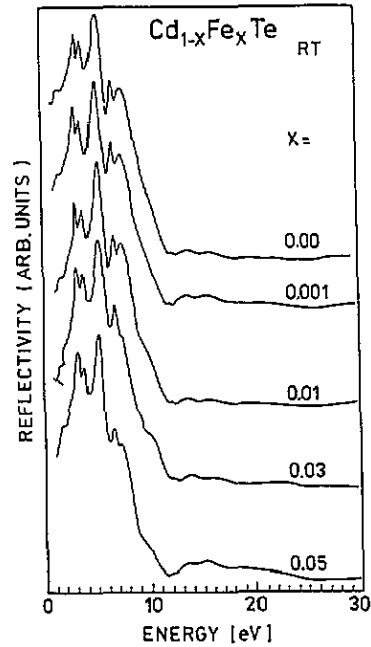**Figure 2.** The reflectivity spectra for $Cd_{1-x}Fe_xTe$ in the 1.0–30.0 eV energy range performed at 300 K (RT).

state [23] (even in the energy gap) to the CB. For the measurements performed at RT, with Fe concentration higher than $x \geqslant 0.001$, the Fe ions cannot be treated as impurities and therefore Szadkowski's analysis [16], made for LNT, should not be directly applied. In $Cd_{1-x}Fe_xTe$ alloys ($x \geqslant 0.001$) the population of the $Fe^{2+/3+}$ deep donor band increases and additionally the number of occupied states at RT because of the thermal excitations, is more than 10^4 times higher than that at LNT. Moreover, at the fundamental absorption edge the depth of light penetration decreases and the influence of the surface recombination processes on the intensity of the photoconductivity current increases. Because of the same method of preparation of our samples we can assume that the velocity of the surface recombination prosesses is similar for all samples. All these effects give access to the photoconductivity maximum of which the energy position E_p shifts only according to the changes of the electronic band structure caused by the different Fe content. Therefore the analysis of the energy position of the E_p maximum as a function of Fe concentration seems to be fairly good, particularly as far as the photoconductivity measurements carried out at RT are concerned.

A review of the literature [22] reveals two trends in the behaviour of the fundamental gap E_g in DMSs, especially in those with Mn. These are (i) a general increase of the energy gap with Mn concentration (at fixed temperature T) and (ii) approximately the same value of E_g extrapolated to $x = 1$, for $A_{1-x}Mn_xTe$ compounds independent of A. Such an E_g is the value of the energy gap for a hypothetical zincblende MnTe compound and A represents different cations such as Cd and Zn [24]. The increase of the energy gap is seen in our reflectivity spectra for $Cd_{1-x}Fe_xTe$, too (figure 4). On the other hand it is clear from the photoconductivity curves that the introduction of a very small amount of Fe ($x = 0.001$) to the host CdTe alters the position of the maximum E_p towards lower energies, while further increasing the Fe content raises the value of E_p (figure 5(b)).

It seems that our experimental results can be consistently explained within the frame
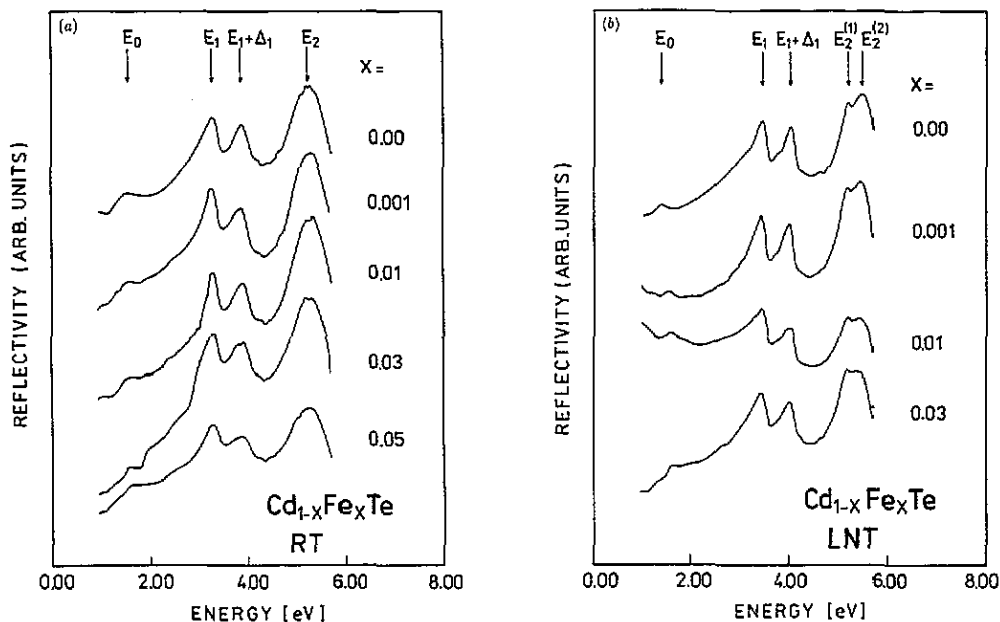
Figure 3. The reflectivity spectra for $Cd_{1-x}Fe_xTe$ in the 1.0–6.0 eV energy range performed (*a*) at 300 K (RT) and (*b*) at 77 K (LNT).
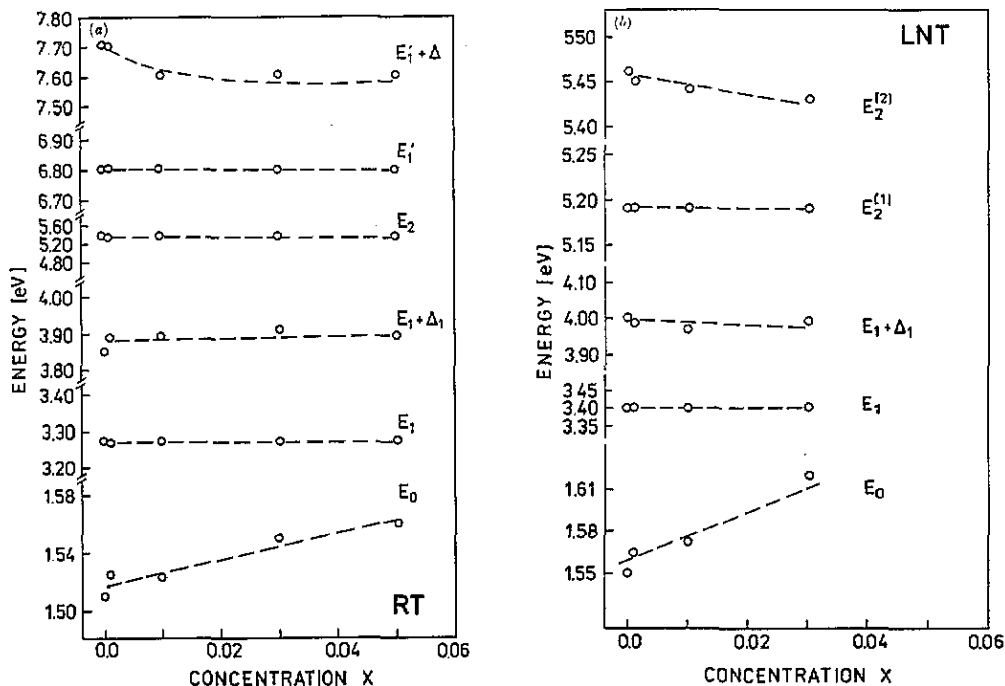

Figure 4. The energy positions of maxima (*a*) E_0, E_1, $E_1 + \Delta_1$, E_2, E_1', and $E_1' + \Delta$ as a function of Fe concentration at 300 K (RT) and (*b*) E_0, E_1, $E_1 + \Delta_1$, $E_2^{(1)}$, and $E_2^{(2)}$ as a function of Fe concentration at 77 K (LNT).
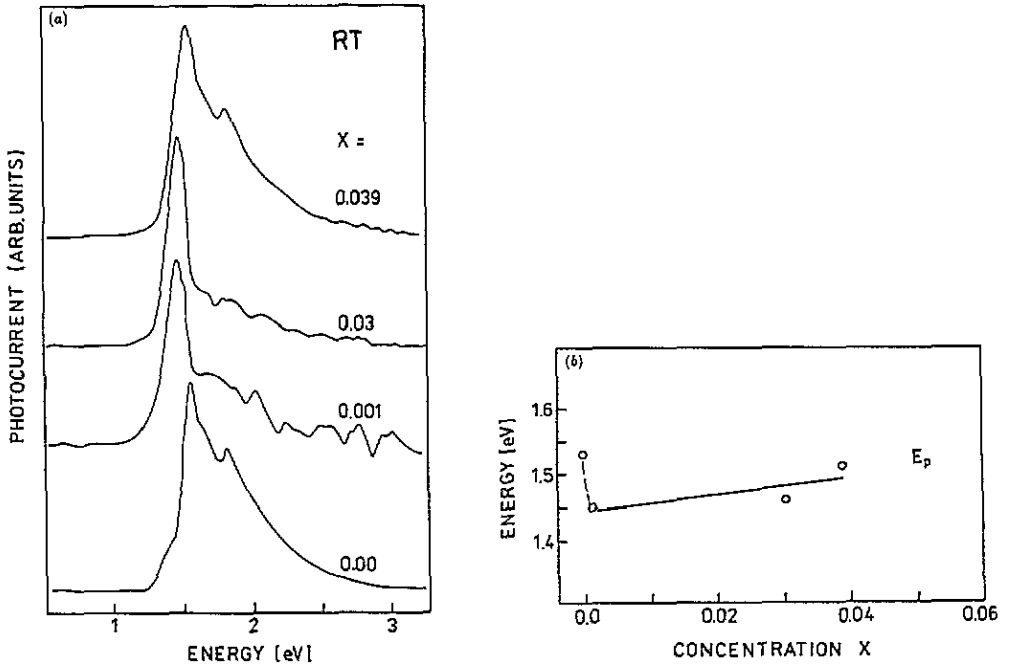
Figure 5. (a) The photoconductivity spectra for mixed crystals $Cd_{1-x}Fe_xTe$ in the 1.0–3.0 eV range. (b) The dependence of the energy position of E_p maximum on the Fe content.

of the previously proposed model of electronic states for these alloys. The existence of the substitutional Fe^{2+} ions in the host CdTe crystal implies the creation of the deep donor-like state above the top of the VB. Since the photoconductivity measurements are sensitive to the excitation of the occupied states existing even in the forbidden energy gap, for the smallest x we observe this deep donor-like state created by Fe, i.e. E_p shifts to lower energies. The further increase of Fe mole fraction causes the bottom of the CB to move up, because the substitution of Cd^{2+} by Fe^{2+} cations results in an increase of E_g (and E_p). E_p shifts to higher energies linearly according to $E_p(x) = (ax + 1.45)$ eV, for $x > 0.00$ (i.e. the point for pure CdTe is excluded), with the slope $a = (1.23 \pm 0.20)$ eV.

The energy position of the E_0 maximum in the reflectivity spectra, representing only the onset of the interband transition between the valence and conduction bands, for Fe content $0.00 \leqslant x \leqslant 0.05$ at RT and LNT increases linearly following $E_0(x) = (bx + 1.52)$ eV where $b = 0.9 \pm 0.20$ eV (figure 4(a)) and $E_0(x) = (bx + 1.56)$ eV where $b = 1.4 \pm 0.30$ eV (figure 4(b)). At RT this slope, within the limit of experimental error, is similar to the slope determined from the photoconductivity measurements. The comparison of the estimated slopes of $E_p(x)$ and $E_0(x)$ curves for photoconductivity and reflectivity data (figures 4(a) and 5(b)) suggests that in both cases the bottom of the CB is the final state of the transitions. The value of 0.08 eV, estimated by us from the photoconductivity measurements (figure 5(b)), for the distance between the donor-like state and the top of the VB, is in fairly good agreement with the interval reported by Lischka *et al* [14]. Moreover, our photoconductivity measurements confirm the excitation scheme $3d^6 \rightarrow 3d^5 + \bar{e}$.

Both experiments can be consistently explained if the model discussed in the introduction is applied [5, 11]. The Fe 3d states, split by the exchange interaction, are further split in the tetrahedral crystal field into a triplet $t_2(\Gamma_{15})$ and a doublet e (Γ_{12}). The t_2 levels are even further split by the spin–orbit (SO) interaction into a singlet Γ_7 and a doublet Γ_8, in the

notation of the double group representation [25]. The spin–down occupied electron state, lying close to the VB maximum, could interact with p-like anion states of Γ_8 symmetry at the top of the VB and because of this interaction the VB of the host crystal is likely to move.

Next, we consider the very well pronounced reflectivity maxima E_1 and $E_1 + \Delta_1$. For $Cd_{1-x}Fe_xTe$ mixed crystals only a small broadening of these maxima is observed but the energy positions remain the same compared to the CdTe structure. Hence, at LNT the reflectivity structure becomes much richer, the $e_1 + \Delta_1$ threshold appears and exhibits similar behaviour to the main E_1 and $E_1 + \Delta_1$ peaks. Taking into account the model discussed, photoemission studies [26] and theoretical calculations [27, 28], we can try to understand the independence of the E_1 and $E_1 + \Delta_1$ energy positions as a function of Fe concentration, both at RT and LNT (figure 4(a) and (b)), respectively. As is well known, the E_1 and $E_1 + \Delta_1$ maxima represent transitions from the SO split valence bands ($L_{4,5}$, L_6) in the vicinity of the L point along the Λ direction ($\langle 111 \rangle$) to the lowest conduction band L_6. On the basis of the calculated band structure of CdTe, the contributions of Cd and Te states near the L point have been already established. Using the LMTO results we can give a quantitative estimate of the contribution of p-like states of Te and Cd of 72% and 20%, respectively, and the contribution of d-like states of Cd of 7% [28]. The photoemission measurements yield information about the contribution of 3d Fe states at ~ 0.6 and 3.6 eV below the top of the VB for $Cd_{1-x}Fe_xTe$ [26]. In the model discussed here, these Fe states should be of the t_2 type. In the zincblende structure the local symmetry of Fe and Te sites is T_d. For the T_d point-group symmetry both the d-like character of the t_2 state (Fe) and the p-like character of the Te electrons are allowed in the representation and, as a result, these orbitals hybridize completely. On the other hand, as has been suggested before, the position in energy of the CB L_6 is likely to be changed by the substitution of Cd^{2+} by Fe^{2+} cations. Therefore we can assume that the interaction in the VB region between d states of Fe and mainly p-like states of Te, as well as possible movement of the lowest CB, may influence the transitions near the L point. This makes E_1 and $E_1 + \Delta_1$ energy positions independent of Fe concentration.

The E_2 maximum placed at 5.4 eV is assigned to several transitions occurring in a large part of the BZ around the Δ and Σ directions. At low temperature (LNT) two components $E_2^{(1)}$ and $E_2^{(2)}$ of E_2 are observed. This corroborates with the results of LMTO calculations performed by Markowski [28]. Both components show broadening with increasing Fe content but $E_2^{(2)}$ shifts in energy whilst $E_2^{(1)}$ does not. This complex situation relates to the circumstances occuring over a volume in the BZ as stated above. The admixture of Fe 3d states over the entire volume in k space may cause cancellation, which leads to the final result of no energy shift.

3.2. The 6–11 eV energy range

In the reflectivity spectra in the ultraviolet region one can distinguish E_1' and $E_1' + \Delta$ maxima (figure 2) related to the transitions between the SO split highest valence band ($L_{4,5}$, L_6) and second conduction bands (L_6, $L_{4,5}$) in the vicinity of the L critical point along the Λ direction [29]. The initial states of these transitions are the same as in the case of E_1 and $E_1 + \Delta_1$ maxima, therefore, one can expect a similar energy dependence. The energy position of the E_1' maximum with increasing Fe content (figure 4(a)) remains almost unchanged as for the E_1 maximum and the explanation of such behaviour suggested above for E_1 and $E_1 + \Delta_1$ maxima seems to be applicable here, as well. However, the energy position of $E_1' + \Delta$ changes in a different way, which should be connected with the nature of final states. Kisiel *et al* [30], using a virtual crystal model for the hypothetical zincblende FeTe for the interpretation of XANES experiments extracted the projected s, p,

and d-like densities of states (DOSs) of FeTe in $Cd_{1-x}Fe_xTe$. They found that the extracted DOSs occupy presumably the bottom of the CB (p-like DOS) and the position 5 eV above it (s, d-like DOS). The latter s- and d-like states could eventually disturb the final state of the interband transitions. The detailed analysis of $E_1 + \Delta_1$ energy positions as a function of Fe concentration indicates as well a small deviation from straight-line dependence.

In the reflectivity structure of pure CdTe near 10.4 eV there is a shoulder associated with the transitions from the third valence band ($L_6^{(2)}$) to the second lowest conduction band ($L_6^{(2)}$), which becomes more visible when the Fe content increases (figure 2). This feature should be connected with the influence of the Fe states in two different regions of the electronic band structure of these compounds. The final state $L_6^{(2)}$ is likely to be disturbed, according to the symmetry of these states, by empty states of FeTe indicated in the XANES experiment [30]. On the other hand from the photoemission data [26] it is known that the 3d state of e-symmetry is placed next to initial state (3.6 eV below the top of the VB). This additional Fe states would be likely to lead to an increase of a joint DOS for the above-mentioned transition to the second lowest conduction band $L_6^{(2)}$.

3.3. The 11–30 eV energy range

There are different explanations in the literature on the origin of the maximum **a** appearing for pure CdTe at about 12.13 eV. Kisiel *et al* [18] interpreted it as a core exciton of the $4d_{5/2}$ level of Cd in contrast to the interpretation of Krause and Gümlich [31] who connected this maximum with a transition from the 5s states of Te. On the other hand, according to the recent (1990) LMTO band-structure calculations [27], the main contribution to peak **a** could come also from the band-to-band transition, i.e. from the two highest valence bands to the fifth conduction band. However, taking into consideration the broadening of the reflectivity maxima depending on the life-time of initial and final states with many-body corrections [32] associated with given transitions the contribution of the band-to-band transition to peak **a** becomes so small [28] that the explanation of the origin of peak **a** as a core exciton should not be excluded. Looking over the behaviour of this maximum in our reflectivity spectra (figure 6), one can notice the independence of its energy position from Fe concentration. Therefore both interpretations, as the core exciton and the band-to-band transition, are possible.

The next maxima **c**, **d**, **e** and **f** (figure 6(*a*)) occur in CdTe at the energies 13.08, 13.77, and 15.63 eV, respectively, with **e** and **f** not separated from each other. Figure 6(*b*) illustrates the shifts in the energy positions of these maxima with changing Fe content. Such similar behaviour is fairly well understood assuming the assignment of these peaks to transitions from the same initial states $d_{5/2}$ of Cd to X_6, DOS, Γ_7 and $L_6^{(2)}$ bands, respectively [18]. The other authors [31–33] associate the **c** reflectivity maximum in pure CdTe with different transitions. Krause and Gümlich [31] assigned it to the core exciton. In all Cd chalcogenides Freeouf [33] found a doublet, **c** and **d** in our notation, split by about 0.6 eV. The fact that the energy of splitting does not change upon going from the sulphide to telluride implies that the splitting is intrinsic to the Cd atom. Moreover, it is in good agreement with the SO splitting of the Cd 4d level in the free atom [34]. This doublet is identified by Freeouf as a $d_{5/2}$ and $d_{3/2}$ band to the CB transition at X_6 lying at about 3.5 eV above the VB maximum. Taking into account Freeouf's results and our data on $Cd_{1-x}Fe_xTe$, both interpretations concerning the maximum **d** seem to be acceptable.

The last two features of reflectivity spectra are the peaks **h** and **i** appearing for the host crystal at 18.8 and 21.4 eV, respectively. The energy positions of both maxima shift linearly with the Fe content although for higher concentration these maxima are undistinguishable.
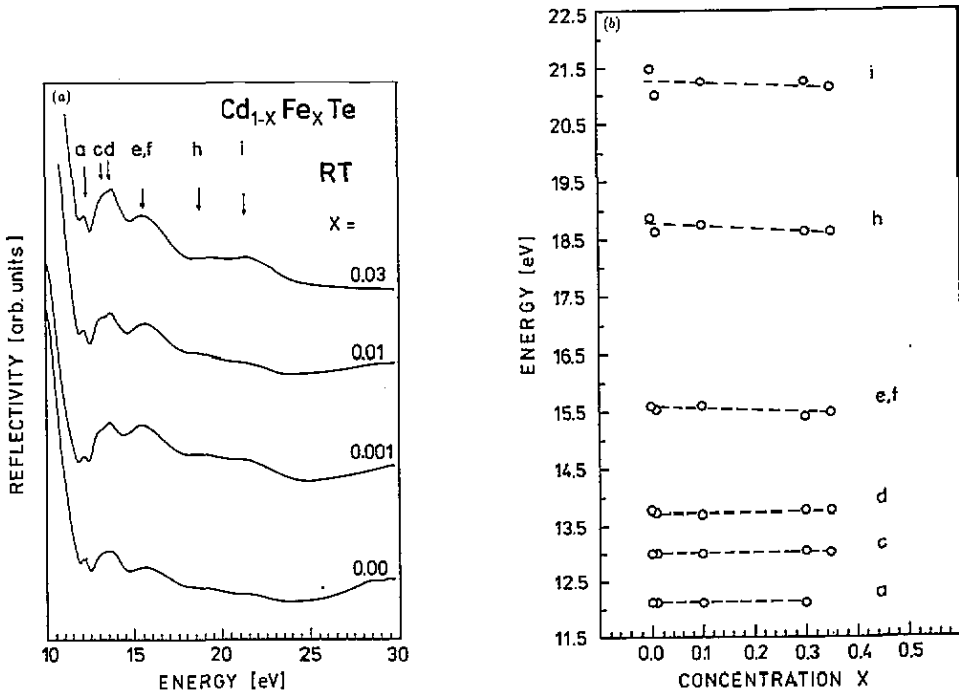
Figure 6. (a) The reflectivity spectra for $Cd_{1-x}Fe_xTe$ in the 10.0–30.0 eV energy range performed at 300 K (RT). (b) The energy positions of maxima **a, c, d, e, f, h** and **i** as a function of Fe concentration.

4. Summary

In this paper, we present the results of the optical studies of mixed crystals $Cd_{1-x}Fe_xTe$ ($0.00 \leqslant x \leqslant 0.05$), representative of the Fe-based DMSs. The reflectivity measurements were carried out in the 1–30 eV energy range at RT and LNT whilst the photoconductivity spectra were taken only in the infrared and visible region at room temperature.

In contrast to $E_0(x)$, which behaves linearly for $0.00 \leqslant x \leqslant 0.05$, the analysis of the energy positions of the main maximum E_p in the photoconductivity spectra as a function of the Fe concentration x shows a jump to lower energy when even a small amount of Fe ions ($x = 0.001$) in the host crystal of CdTe appears. A further increase of Fe concentration causes the linear dependence $E_p(x)$. The slopes of $E_p(x)$ and $E_0(x)$ taken from the reflectivity measurements are almost the same within experimental error. These results indicate the existence of the deep donor-like state, predicted by the band-structure model [5, 11] of Fe-based DMSs, localized near the top of the VB. Using the photoconductivity data the value of 0.08 eV above the top of the VB for the energy position of this deep donor-like state was found. This is in good agreement with the photo-EPR results [14]. In the frame of the model mentioned above the influence of $Fe^{2+}(3d^6)$ states and their s–p–d hybridization with the bands of the host crystal has been analysed. The changes in the shape and the energy positions of the reflectivity maxima connected with the interband transitions E_0, E_1, $E_1 + \Delta_1$, E_2, E_1', and $E_1' + \Delta$ as well as core-level (**c, d, e, f, h** and **i**) excitations have been discussed in detail.

Acknowledgments

References

[1] Furdyna J K 1982 *J. Appl. Phys.* **53** 7637
[2] Mycielski A 1988 *J. Appl. Phys.* **63** 3279
[3] Joshi N V and Mogollón L 1986 *Prog. Cryst. Growth Charact.* **10** 65
[4] Kisiel A, Rodzik A, and Giriat W 1985 *5th Gen. Conf. Condens. Matter Division EPS (Berlin); Europhys. Conf. Abstracts* ed D H Haberland and J Treusch (Geneva: European Physical Society) pp PFr-4-057
[5] Sarem A, Kowalski B J and Orłowski B A 1990 *J. Phys. C: Solid State Phys.* **2** 8173
[6] Sarem A, Kowalski B J, Majewski J, Górecka J Orłowski B A, Mycielski A and Jezierski K 1990 *Acta Phys. Polon.* A **77** 407
[7] Kowalski B J, Sarem A and Orłowski B A 1990 *Phys. Rev.* B **42** 5159
[8] Chadi D J, Walter J P, Cohen M L, Petroff J and Balkański M 1972 *Phys. Rev.* B **5** 3058
[9] Chelikowsky J R and Cohen M L 1976 *Phys. Rev.* B **14** 556
[10] Taniguchi M, Ley L, Johnson R L, Ghijsen J and Cardona M 1986 *Phys. Rev.* B **33** 1206
[11] Kisiel A, Piacentini M, Antonangeli F, Zema N and Mycielski A 1989 *Solid State Commun.* **70** 693
[12] Taniguchi M, Ueda Y, Morisada I, Murashita Y, Ohta T, Souma I and Oka Y 1990 *Phys. Rev.* B **41** 3069
[13] Mycielski A, Dzwonkowski P, Kowalski B, Orłowski B A, Dobrowolska M, Arciszewska M, Dobrowolski W and Baranowski J M 1986 *J. Phys. C: Solid State Phys.* **19** 3605
[14] Lischka K, Brunthaler G and Jantsch W 1985 *J. Cryst. Growth* **72** 355
[15] Jantsh W, Brunthaler G and Hendorfer G 1986 *Defects in Semiconductors* vols 10–12, ed H J von Barbelen (Materials Science Forum) pp 515–20
[16] Szadkowski A J 1990 *J. Phys.: Condens. Matter* **2** 9853
[17] Oleszkiewicz J, Podgórny M, Knapik J and Kisiel A 1985 *Opt. Appl.* **15** 163
[18] Kisiel A, Zimnal-Starnawska M, Antonangeli F, Piacentini M and Zema N 1986 *Nuovo Cimento* D **8** 436
[19] Kendelewicz T 1980 *Solid State Commun.* **36** 127
[20] Zimnal-Starnawska M, Pogórny M, Kisiel A, Giriat W, Demianiuk M and Żmija J 1984 *J. Phys. C: Solid State Phys.* **17** 615
[21] Kisiel A, Piacentini M, Antonangeli F, Oleszkiewicz J, Rodzik A, Zema N and Mycielski A 1987 *J. Phys. C: Solid State Phys.* **20** 5601
[22] Becker W M 1988 *Semiconductors and Semimetals* vol 25, ed J K Furdyua and J Kossut (Boston, MA: Academic) pp 35–72
[23] Marfaing Y 1980 *Handbook on Semiconductors* ed T S Moss; vol 2, ed M Balkanski (Amsterdam: North-Holland) p 417
[24] Lee Y R, Ramdas A K and Aggarwal R L 1988 *Phys. Rev.* B **38** 10 600
[25] Miller A, MacKinnon A and Weaire D 1981 *Solid State Physics* vol 36, ed H Ehrenreich, F Seitz and D Turnbull (New York: Academic) p 167
[26] Orłowski B J, Fraxedas J, Denecke R, Kowalski B J, Mycielski A and Ley L 1990 *Acta Phys. Polon.* A **79** 355
[27] Markowski R and Podgórny M 1990 *J. Phys.: Condens. Matter* **3** 9041
[28] Markowski R 1991 private communication
[29] Rodzik A and Kisiel A 1983 *J. Phys. C: Solid State Phys.* **16** 203
[30] Kisiel A, Lee P M, Burattini E, Dalba G, Fornasini P and Giriat W 1991 *J. Appl. Phys.* **69** 6119
[31] Krause K and Gümlich H E 1988 *Phys. Rev.* B **37** 6336
[32] Müller J E, Jepsen O and Wilkins J W 1982 *Solid State Commun.* **42** 365
    Müller J E and Wilkins J W 1984 *Phys. Rev.* B **29** 4331
[33] Freeouf J L 1973 *Phys. Rev.* B **7** 3810
[34] Herman F and Skilman S 1963 *Atomic Structure Calculations* (Englewood Cliffs, NJ: Prentice Hall) pp 2–9